Pion and kaon condensation in a 3-flavor Nambu–Jona-Lasinio model

A. Barducci,* R. Casalbuoni,† G. Pettini,‡ and L. Ravagli§

Department of Physics, University of Florence, Florence, Italy
and INFN Sezione di Firenze, Via G. Sansone 1, I-50109, Sesto F.no, Firenze, Italy
(Received 19 October 2004; published 24 January 2005)

We analyze the phase diagram of a 3-flavor Nambu–Jona-Lasinio model at finite temperature T and chemical potentials μ_u, μ_d, μ_s. We study the competition of pion and kaon condensation and we propose a physical situation in which kaon condensation could be led only by light quark finite densities.

I. INTRODUCTION

In the last few years the study of QCD at finite temperature and densities has been a subject of great interest. In particular, the regime of high temperatures and moderate densities is relevant for the physics of heavy ion collisions: the presence of a tricritical point, suggested in [1] is significant to determine the transition from a quark-gluon plasma (QGP) phase to a hadronic phase [2].

Moreover, the presence of an isospin chemical potential, namely, of an asymmetry in the densities of light quarks, could complicate this picture: for values of $\mu_I = (\mu_u - \mu_d)/2$ attainable in the experiments, it is expected that the critical lines associated to the light flavors, and therefore the ending points, are mutually shifted (however the presence of instanton effects could modify this picture, as discussed in Ref. [3]). The presence of two critical lines would make the transition smoother and would produce observable effects on physical quantities across the transition [4,5].

On the other hand, the regime of low temperature and high densities is relevant for compact stars. The existence of stars whose core is so dense that quarks can be treated as fundamental degrees of freedom has been considered for instance in [6]: there, the temperature is small enough to safely consider the limit $T \to 0$. In this context, the physical scenario is very rich and interesting. For quark chemical potentials higher than $400 \div 500$ MeV, the presence of superconductive phases has been established [7]: there, the mass of the strange quark plays the role of distinguishing the pattern of symmetry breaking between a 2-flavor superconductive (2SC) and a 3-flavor color flavor locking (CFL) phase, in both cases the gap being of the order of a few tens of MeV. For this reason, an exhaustive study of these phenomena must take into account the strange quark sector. It is also worth to mention that taking into account

weak equilibrium and color and electric neutrality many other interesting superconductive phases could exist [8–11].

The study of finite density on lattice has well-known problems and except for the attempt of Fodor and Katz in Ref. [12] the only studied case is the one corresponding to low densities [13]. For this reason, the only tool available at this moment for the study of the phase diagram in the range from medium to high densities is a class of effective models: the stability of the results obtained with different approaches must be checked to give predictivity to the analyses.

In any case, at zero temperature for values of $\mu_I \geq m_\pi/2$ a pion condensed phase should appear, as has been first suggested by [14] in the framework of a chiral model: this phase is confirmed by lattice analyses [15], directly investigable since for $\mu_I \neq 0$ and $\mu_B = 0$ the fermion determinant is positive, within chiral models [16] and within microscopical models [3,4,17–19]. Our previous study in the NJL model [19] and that in Ref. [3], together with the one in random matrix [17], showed the effect of both isospin and baryon chemical potentials on the structure of the QCD phase diagram.

By extending this analysis to the third flavor, a kaon condensed phase is expected in the region of high strange quark chemical potential $\mu_s \geq m_K$, as shown by Ref. [20]. In the latter analysis being realized in the context of chiral models at zero temperature, it would be interesting to study the competition between pion and kaon condensation in the framework of a microscopical model, for a general configuration in the space of thermodynamical parameters (T, μ_u, μ_d, μ_s).

Moreover, it has been suggested a kaon condensed phase in the context of high density nuclear matter [21] and, more recently, in particular, in the CFL regime [22]: since we do not yet know whether the densities attainable in the core of a neutron star can be high enough to favor a superconductive phase, we study here the possibility of kaon condensation when neglecting diquark condensates, and where the densities are mainly associated to light quarks. Also, for the first time we

*Electronic address: barducci@fi.infn.it
†Electronic address: casalbuoni@fi.infn.it
‡Electronic address: pettini@fi.infn.it
§Electronic address: ravagli@fi.infn.it

perform the study of kaon condensation by using a micro-scopical model.[1]

To summarize, in this paper we study pion and kaon condensation at finite temperature and quark densities, by using a 3-flavor nonlocal Nambu–Jona-Lasinio (NJL) model, and we propose a physical scenario in which kaon condensation could be driven only by a light quark finite density. The possibility of a kaon condensation at $\mu_s = 0$ could be important in the context of neutron stars, where, by neglecting electroweak effects, the densities are associated only to light quarks. To this end, we generalize our analyses previously performed in the 2-flavor sector [18,19]. In this paper we turn off the electroweak effects and we do not consider the possibility of di-quark con-densation; therefore, our results will be reliable only in the regime of intermediate densities (with chemical potentials lower than $400 \div 500$ MeV). Moreover, we neglect the presence of instanton effects that could modify the struc-ture of phase diagrams.

II. THE MODEL

Our purpose is to explore the general structure of the phase diagram for chiral symmetry and pion and/or kaon condensation in 3-flavor QCD at nonzero quark densities and its evolution in temperature, by using an effective model with quark degrees of freedom. To this end, we employ the Nambu–Jona-Lasinio model with a form factor included so as to imply a decreasing of the fermion self-energy at high momenta [24]. In this way we generalize, to 3 flavors, previous works concerning the simpler 2-flavor case [18,19] which were inspired by Ref. [4] where the authors had only considered the case of small differences between the u and d quark chemical potentials. A complete study of the 2-flavor phase diagram in the space of tem-perature T, baryon and isospin chemical potentials μ_B, μ_I was first done in the context of a random matrix model [17]. To our knowledge, so far the only study of meson condensation in the general case of 3-flavor QCD is based on a chiral Lagrangian [20]. Nevertheless the use of a model such as the NJL model or *ladder* QCD [25] is necessary if we want to include the effects of a net baryon charge and also study chiral symmetry restoration through the behavior of scalar condensates, besides the pseudosca-lar ones. This is not possible within a chiral Lagrangian approach. As we already stressed in Ref. [19], ladder QCD and the version of the NJL model we use in the present work are very similar. Actually the main difference is that in ladder QCD the quark self-energy depends on the four-momentum whereas in the extended NJL model it depends only on the three-momentum. This feature greatly simpli-

fies the numerical calculations and this is the reason why we employ the NJL model instead of ladder QCD.

Let us thus start with the Lagrangian of the NJL model with three flavors u, d, s, with current masses $m_u = m_d \equiv m$ and m_s and chemical potentials μ_u, μ_d, μ_s, respectively

$$\mathcal{L} = \mathcal{L}_0 + \mathcal{L}_m + \mathcal{L}_\mu + \mathcal{L}_{\text{int}}$$

$$= \bar{\Psi} i \hat{\partial} \Psi - \bar{\Psi} M \Psi + \Psi^\dagger A \Psi + G \sum_{a=0}^{8} [(\bar{\Psi} \lambda_a \Psi)^2$$

$$+ (\bar{\Psi} i \gamma_5 \lambda_a \Psi)^2], \qquad (1)$$

where

$$\Psi = \begin{pmatrix} u \\ d \\ s \end{pmatrix}, \qquad A = \begin{pmatrix} \mu_u & 0 & 0 \\ 0 & \mu_d & 0 \\ 0 & 0 & \mu_s \end{pmatrix},$$

$$M = \begin{pmatrix} m & 0 & 0 \\ 0 & m & 0 \\ 0 & 0 & m_s \end{pmatrix}.$$

M is the quark current mass matrix which is taken diagonal and A is the matrix of the quark chemical poten-tials. As usual $\lambda_0 = \sqrt{\frac{2}{3}} \mathbf{I}$ and λ_a, $a = 1, ..., 8$ are the Gell-Mann matrices. For $M = 0$ and $A = 0$ or $A \propto \mathbf{I}$, the Lagrangian is $U(3)_L \otimes U(3)_R$ invariant. The chiral symme-try is broken by $M \neq 0$ which also breaks $SU(3)_V$ down to $SU(2)_V$ as $m \neq m_s$. However, this symmetry is also lost, since we generally consider $\mu_u \neq \mu_d$. The remaining symmetry is thus the product of three independent phase transformations $U_u(1) \otimes U_d(1) \otimes U_s(1)$. In this applica-tion, we do not consider the 't Hooft determinant, that explicitly breaks $U(1)_A$. Also, we do not take into account the possibility of a di-fermion condensation, which is relevant at low temperatures and high densities, and will be analyzed in a forthcoming publication: for this reason, we limit the validity of our study up to quark chemical potentials of order of $400 \simeq 500$ MeV.

We note that we can express $\mathcal{L}_\mu$ either by using the variables μ_u, μ_d, μ_s or by introducing an averaged light quark chemical potential

$$\mu_q = (\mu_u + \mu_d)/2 \qquad (2)$$

and the three combinations

$$\mu_B = (\mu_u + \mu_d + \mu_s)/3; \qquad \mu_I = (\mu_u - \mu_d)/2;$$
$$\mu_Y = (\mu_q - \mu_s)/2 \qquad (3)$$

which couple to charge densities proportional to the baryon number, to the third component of isospin and to hyper-charge, respectively,

$$\mathcal{L}_\mu = \mu_B \Psi^\dagger \Psi + \mu_I \Psi^\dagger \lambda_3 \Psi + \frac{2}{\sqrt{3}} \mu_Y \Psi^\dagger \lambda_8 \Psi. \qquad (4)$$

---

[1] In Ref. [23] a study of meson properties at finite quark densities within the NJL model is performed. However, they do not deal with meson condensation.

To study whether a pion and/or kaon condensate is formed, we need to calculate the effective potential. This is obtained by using the standard technique to introduce bosonic (collective) variables through the Hubbard-Stratonovich transformation and by integrating out the fermion fields in the generating functional. The one-loop effective potential we get is:

$$V = \frac{\Lambda^2}{8G}(\chi_u^2 + \chi_d^2 + \chi_s^2 + 2\rho_{ud}^2 + 2\rho_{us}^2 + 2\rho_{ds}^2) + V_{\log},$$
(5)

$$V_{\log} = -\frac{1}{\beta}\sum_{n=-\infty}^{n=+\infty}\int\frac{d^3p}{(2\pi)^3}\operatorname{tr}\,\log\begin{pmatrix} h_u & -\gamma_5 F^2(\vec{p})\Lambda\rho_{ud} & -\gamma_5 F^2(\vec{p})\Lambda\rho_{us} \\ \gamma_5 F^2(\vec{p})\Lambda\rho_{ud} & h_d & -\gamma_5 F^2(\vec{p})\Lambda\rho_{ds} \\ \gamma_5 F^2(\vec{p})\Lambda\rho_{us} & \gamma_5 F^2(\vec{p})\Lambda\rho_{ds} & h_s \end{pmatrix},$$

$$h_f = (i\omega_n + \mu_f)\gamma_0 - \vec{p}\cdot\vec{\gamma} - [m_f + F^2(\vec{p})\Lambda\chi_f],$$
(6)

where the form factor $F(\mathbf{p}^2) = \frac{\Lambda^2}{\Lambda^2+\mathbf{p}^2}$ (Λ is a mass scale) has been introduced to mimic asymptotic freedom as in Refs. [24]. In Eq. (6) tr means sum over Dirac, flavor and color indices, and ω_n are the Matsubara frequencies. The dimensionless fields χ_f and $\rho_{ff'}$ are connected to the condensates by the following relations

$$\chi_f = -4G\frac{\langle\bar{\Psi}_f\Psi_f\rangle}{\Lambda},$$

$$\rho_{ff'} = -2G\frac{\langle\bar{\Psi}_f\gamma_5\Psi_{f'} - \bar{\Psi}_{f'}\gamma_5\Psi_f\rangle}{\Lambda}$$
(7)

and are variationally determined at the absolute minimum of the effective potential. Following the analyses performed within the chiral Lagrangian approach [14,20], we expect a superfluid phase with condensed pions when the isospin chemical potential exceeds a critical value μ_I^C ($\mu_I^C = m_\pi/2$ at $T = 0$); analogously a kaon condensation phase is expected when μ_Y, which measures the unbalance between the light quarks average chemical potential μ_q and μ_s, is high enough. For $\mu_u = \mu_d$ and $T = 0$ this limit is $\mu_Y^C = m_K/2$.

To fix the free parameters of the model, which are Λ, the average light quark and the strange quark masses m, m_s and the coupling $G = g/\Lambda^2$, we calculate the charged pion and kaon masses (by fixing their decay constants to the experimental values) and the light quark scalar condensate in the vacuum.

By choosing the free parameters as follows

$$\Lambda = 1000 \text{ MeV}; \qquad g = G\Lambda^2 = 6; \qquad m = 1.7 \text{ MeV};$$

$$m_s = 42 \text{ MeV}$$
(8)

we get for the light quark condensate, the constituent light quark mass, the pion mass, and the kaon mass, respectively, the results $\langle\bar{\Psi}_f\Psi_f\rangle = -(252 \text{ MeV})^3$, $M_q = 385 \text{ MeV}$, $m_\pi = 142 \text{ MeV}$, $m_K = 500 \text{ MeV}$. Furthermore, we find the expected agreement between $m_\pi/2$ and μ_I^C (within 1%), and also between μ_Y^C and $m_K/2$ (within 4%).

The very low value we find from our fit for the quark masses is entirely due to the choice of form factors (instantaneous approximation), see [26], but their ratio $m_s/m \simeq 25$ is in agreement with the value given by the ratio of the pseudoscalar masses.

III. PHASE DIAGRAM FOR CHIRAL SYMMETRY AND MESON CONDENSATION

As usual, we determine the phases of the model by looking at the absolute minimum of the effective potential, given in Eqs. (5), (6). Since there are four thermodynamical parameters, namely T, μ_u, μ_d, μ_s (or T, μ_B, μ_I, μ_Y), we start from $T = 0$ and then follow the evolution in temperature of two-dimensional slices in the space of chemical potentials. We recall that the global symmetry in the model is given by the product of three U(1) groups. The possible formation of a nonzero value of one of the pseudoscalar fields $\rho_{ff'}$ implies the spontaneous breaking of a U(1) symmetry with the appearance of a Goldstone boson. The transition to this superfluid phase leaves two U(1) groups unbroken and between them there is always the U(1)$_V^B$. For instance, the formation of a ρ_{ud} condensate implies the breaking of the U(1)$_V^I$ symmetry, whereas U(1)$_V^Y \otimes$ U(1)$_V^B$ are left unbroken. At the threshold one of the charged pions, depending on the sign of μ_I, is the Goldstone boson, whereas the other mesons of the octet remain massive (see also [20]).

Thus we characterize different regions of pion or kaon condensation with the pseudoscalar field which acquires a nonvanishing vacuum expectation value (v.e.v.), whereas the other v.e.v.'s are vanishing. Then, to facilitate the physical interpretation and to directly compare it with the results of Ref. [20], in the pictures we label these regions directly with the symbol of the particle that condenses, rather than with that of the corresponding field $\rho_{ff'}$. The scalar fields χ_f do not break any symmetry as chiral symmetry is explicitly broken by the current quark masses. However these fields undergo crossover or discontinuous transitions for given values of the thermodynamical parameters. Thus we distinguish between regions where a nonzero v.e.v. of a scalar field is primarily due to dynamical effects, and we indicate them with the relative symbol χ_f, from regions where their values are of order $\sim m_f/\Lambda$, where we put no symbol. We also avoid putting the symbol
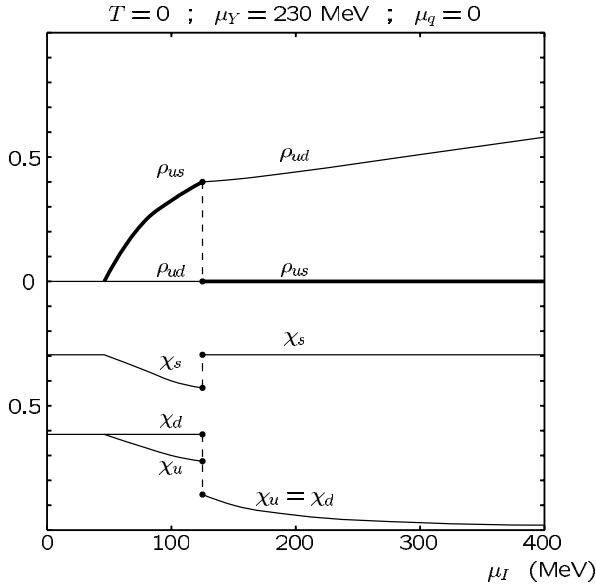
χ_f in a region where the pseudoscalar field associated with that flavor starts to form, and χ_f is not yet of order $\sim m_f/\Lambda$. Furthermore, both for pseudoscalar meson condensation and for the transitions associated with scalar fields, the boundaries of the regions separated by discontinuous transitions are represented by solid lines whereas dashed lines indicate continuous transitions. To start with, we set $\mu_u = -\mu_d$, which is the case studied by Toublan and Kogut in Ref. [20]. However, to compare our results with theirs, we have to remark that we adopt different combinations of the microscopic chemical potentials μ_u, μ_d, μ_s. In this case, where $\mu_q = 0$ (see Eq. (2)), we plot the phase diagram in the plane of μ_Y and μ_I, which are proportional, respectively, to μ_s and to $\mu_u - \mu_d$ and which correspond to half of the chemical potentials employed in Ref. [20]. In Fig. 1 we plot the quadrant with $\mu_Y > 0$, $\mu_I > 0$ of the phase diagram at zero temperature. Let us start by looking at what happens by moving along the vertical line at $\mu_I = 0^+$, where 0^+ stands for an infinitesimally small positive value, in order to remove the degeneracy between K^+ and K^0. In this case one starts from a "normal" phase (see also Ref. [20]) characterized by chiral symmetry breaking by large scalar condensates and then, for $\mu_Y \simeq m_K/2 \simeq 250$ MeV, the scalar χ_u and χ_s condensates smoothly rotate into a ρ_{us} condensate, whereas the χ_d field remains unchanged across the transition. We have indicated in the picture this new region with the symbol $\langle K^+\rangle$ (rather than with ρ_{us}) as with these signs of the chemical potentials it is the positively charged

kaon to condense. By further increasing μ_Y the dynamical effect associated with the strange quark condensation is weakened by a high strangeness density and the favored phase becomes that with $\chi_s \sim m_s/\Lambda$ and large χ_u, χ_d. The kaon condensate vanishes in this case through a first order transition. The same situation hereby described also holds when we move along vertical lines with $\mu_I \lesssim m_\pi/2$, with a linear decrease of the critical μ_Y for kaon condensation and a weak linear increase for the second transition at higher μ_Y. On the other hand, when we move along the horizontal line at $\mu_Y = 0$ and we increase μ_I, we pass from the normal phase to a pion condensation phase (in this case the π^+) described by a finite ρ_{ud}, whereas χ_s remains large. This situation was already known by the previous studies of the 2-flavor NJL model [19]. This transition is also second order. This situation persists at larger μ_I too. In the intermediate regions there is a competition between pion and kaon condensation. For instance, by fixing $\mu_I \gtrsim m_\pi/2$, starting from low μ_Y in the π^+-condensed phase with a large χ_s and increasing μ_Y,[2] we find that the system goes to the phase where the K^+ condenses when $\mu_Y \gtrsim m_K/2$. Consequently χ_s becomes $\sim m_s/\Lambda$ whereas χ_d becomes large (if $\mu_I < 325$ MeV) and the full transition is discontinuous. When μ_Y is about 300 MeV (with a linear weak increase for growing μ_I), the kaon condensate vanishes and a pion condensed phase shows up, with all the scalar condensates $\chi_f \sim m_f/\Lambda$. The transition is first order. Finally, for high μ_I and μ_Y in the range of values corresponding to kaon condensation, there is a phase analogous to the previous one, with a kaon condensate instead of a pion condensate and $\chi_f \sim m_f/\Lambda$. This region is connected to the others through discontinuous transitions too.

In Fig. 2 we plot the behavior of the scalar and pseudoscalar condensates vs μ_I at $\mu_q = 0$, $\mu_Y = 230$ MeV, and $T = 0$ corresponding in Fig. 1 to the path marked by the solid line a. It is worth remarking the rotation of the χ_u and χ_s fields into a ρ_{us} field at the continuous transition for kaon condensation (at $\mu_I \simeq 50$ MeV) and the further "exchange" of the two pseudoscalar fields ρ_{us} and ρ_{ud} at the pion condensation transition (at $\mu_I \simeq 125$ MeV).

In Fig. 3 we plot the behavior of the scalar and pseudoscalar condensates vs μ_Y at $\mu_q = 0$, $\mu_I = 200$ MeV, and $T = 0$ (following the path of the solid line b in Fig. 1).

In Fig. 4 the phase diagram of Fig. 1 is extended to negative values of μ_I and μ_Y too. This picture is thus simply obtained by reflection of Fig. 1 around its axes at $\mu_Y = 0$ and $\mu_I = 0$. The only difference is that in the other three quadrants different pseudoscalar mesons of the octet condense (see also Ref. [20]).

The evolution of the scalar fields for growing temperatures is well known. In particular, as expected the growth of

FIG. 1. Phase diagram for chiral symmetry restoration and meson condensation in the plane (μ_I, μ_Y) at $\mu_q = 0$ and $T = 0$. Different regions are specified by the nonvanishing of a given condensate, whereas the others are vanishing (ρ_{ud}, ρ_{us}) or order $\sim m_f/\Lambda$ (χ_u, χ_d, χ_s). Dashed lines are for the continuous vanishing of pseudoscalar fields, whereas solid lines are for discontinuous behaviors. The solid lines a and b refer to specific paths at fixed values of $\mu_Y = 230$ MeV (line a) and $\mu_I = 200$ MeV (line b).

---

[2]In this case, working at $\mu_q = 0$, it simply means to increase $|\mu_s|$.

$T = 0$; $\mu_Y = 230$ MeV ; $\mu_q = 0$

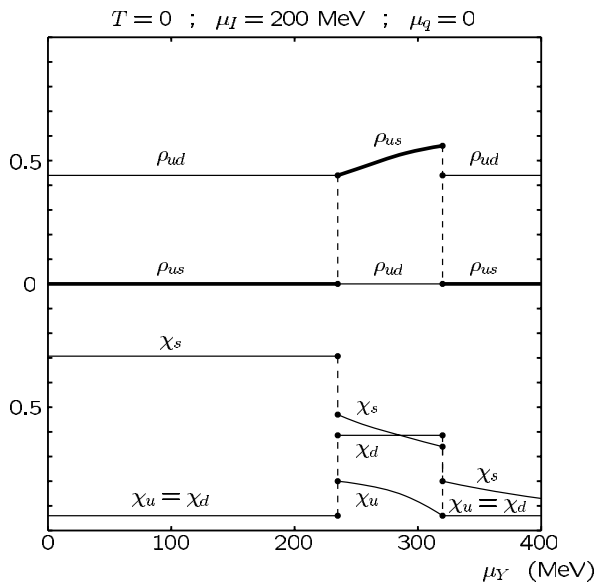FIG. 2. Scalar and pseudoscalar condensates vs μ_I, for $T = 0$, $\mu_q = 0$, and $\mu_Y = 230$ MeV. The path followed in the phase diagram of Fig. 1 is that of the solid line a.

temperature fights against pion and kaon condensation. We find that the kaon condensed phase disappears at $\mu_I = 0$ for $T > 85$ MeV. In Fig. 5 we show the evolution of the phase diagram of Fig. 1 at $T = 100$ MeV. The region for kaon condensation has shrunk and the transitions associated with chiral symmetry approximate restoration have become continuous. Above $T \simeq 110$ MeV the regions of kaon condensation disappear. In Fig. 6 we plot the further evolution of the phase diagram of Fig. 1 at $T = 140$ MeV.

$T = 0$; $\mu_I = 200$ MeV ; $\mu_q = 0$

FIG. 3. Scalar and pseudoscalar condensates vs μ_Y, for $T = 0$, $\mu_q = 0$, and $\mu_I = 200$ MeV. The path followed in the phase diagram of Fig. 1 is that of the solid line b

$T = 0$; $\mu_q = 0$
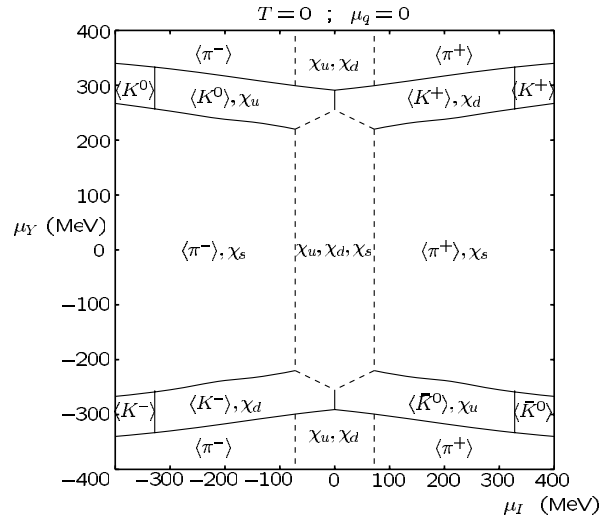
FIG. 4. Phase diagram for chiral symmetry restoration and meson condensation in the plane (μ_I, μ_Y) at $\mu_q = 0$ and $T = 0$. Different regions are specified by the nonvanishing of a given condensate, whereas the others are vanishing ($\rho_{ud}, \rho_{us}, \rho_{ds}$) or order $\sim m_f/\Lambda$ (χ_u, χ_d, χ_s). Dashed lines are for the continuous vanishing of pseudoscalar fields, whereas solid lines are for discontinuous behaviors.

In the range of values of μ_I, μ_Y that we have considered, only the regions of pion condensation and the usual regions with chiral symmetry breaking separated by continuous transitions from analogous phases with $\chi_s \sim m_s/\Lambda$ for
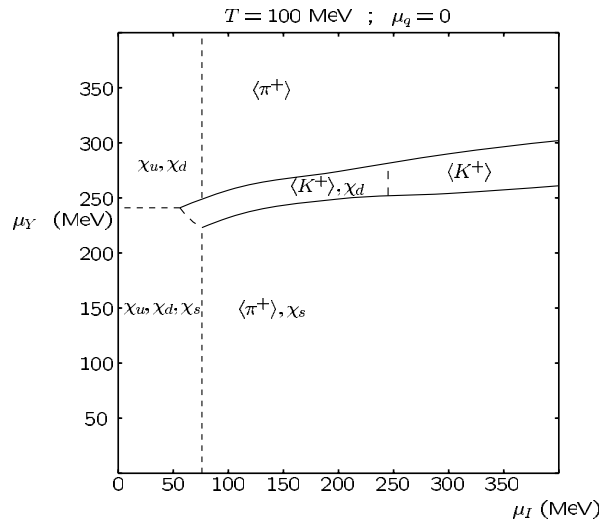
$T = 100$ MeV ; $\mu_q = 0$

FIG. 5. Phase diagram for chiral symmetry restoration and meson condensation in the plane (μ_I, μ_Y) at $\mu_q = 0$ and $T = 100$ MeV, which is above the temperature of the tricritical point. Different regions are specified by the nonvanishing of a given condensate, whereas the others are vanishing (ρ_{ud}, ρ_{us}) or order $\sim m_f/\Lambda$ (χ_u, χ_d, χ_s). Dashed lines are for the continuous vanishing of pseudoscalar fields or for crossover transitions for scalar fields, whereas solid lines are for discontinuous behaviors.
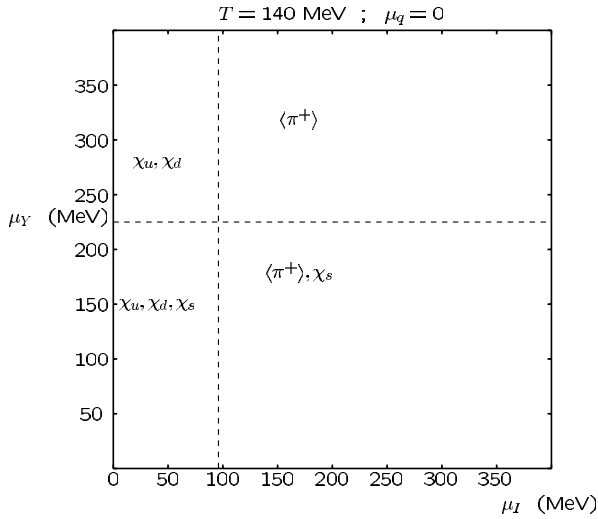
FIG. 6. Phase diagram for chiral symmetry restoration and pion condensation in the plane (μ_I, μ_Y) at $\mu_q = 0$ and $T = 140$ MeV, which is above the highest temperature ~ 110 MeV to have kaon condensation. Different regions are specified by the nonvanishing of a given condensate, whereas the others are vanishing (ρ_{ud}) or order $\sim m_f/\Lambda$ (χ_u, χ_d, χ_s). Dashed lines are for the continuous vanishing of pseudoscalar fields or for crossover transitions for scalar fields.

large μ_Y remain. Finally, pion condensation disappears above the crossover critical temperature $T = 192$ MeV.

IV. KAON CONDENSATION IN THE REGION OF HIGH μ_q

So far we have considered $\mu_u = -\mu_d$ (and thus $\mu_q = 0$). Besides this case, the relevant features of the full phase diagram can be grasped by considering two other possibilities, which are $\mu_u = \mu_d$ (and thus $\mu_I = 0$), and $\mu_s = 0$, which has been already considered in Ref. [19]. In this section, we suggest a hypothesis for a kaon condensation driven mainly by light quark finite densities, with μ_s low or even zero. We recall that in the case of $\mu_s = 0$ there is an equal number of strange quarks and antiquarks, and in that case kaon condensation would concern a light particle (antiparticle), associated to the external field, and a strange antiquark (quark) belonging to the sea. In Ref. [19], we had not inserted the pseudoscalar fields with strangeness content: the possibility of kaon condensation at $\mu_s = 0$ would modify the phase diagram in the (μ_u, μ_d) plane of Ref. [19] with the insertion of regions with condensed kaons. However, except for this, no further modification would be necessary, whereas the possibility of kaon condensation at zero or low values of μ_s can be also studied for $\mu_I = 0$, which is therefore the last situation we examine. From its definition in Eq. (3), we see that μ_Y measures the difference between the strange quark chemical potential and μ_q (which at $\mu_I = 0$ is the chemical potential associated with one of the light flavors) similarly to μ_I which measures the unbalance between the u and d quark

chemical potentials. Therefore as pion condensation can occur, at $T = 0$ and for instance at $\mu_d = 0$, when $\mu_u \gtrsim m_\pi$, similarly we could expect a kaon condensed phase at $T = 0$ and $\mu_s = 0$ when $\mu_q \gtrsim m_K$. However, within our approximations, this does not happen, the reason being that m_K is higher than the critical value of μ_q for the melting of the dynamical part of $\langle \bar{\Psi}_f \Psi_f \rangle$, $f = u, d$. In other words, when the condensates of the light quarks start to decrease to values $\sim m/\Lambda$, the effective kaon mass starts to increase and kaon condensation always remains unfavored (the same does not happen at $\mu_q = 0$ because the melting of the dynamical part of $\langle \bar{s}s \rangle$ occurs at higher values of μ_s and actually we find kaon condensation as shown in the last section). Nevertheless, since we do not have taken into account the effects of di-quark condensates which could break chiral symmetry, it would be interesting to further analyze what happens with their inclusion. We will analyze this case in further work.

For the time being, let us show, in Fig. 7, the $T = 0$ phase diagram in the (μ_q, μ_s) plane at $\mu_I = 0^-$, where 0^- stands for an infinitesimally small negative value, which is necessary to decide which are the kaons that condense (in any case, within a neutron star a finite negative isospin chemical potential is present). The structure of this phase diagrams recalls that of [19] for pion condensation in the (μ_u, μ_d) plane, with a normal phase in the middle, characterized by high values of the scalar condensates χ_u, χ_d, χ_s. This phase is separated from the regions of chiral symmetry approximate restoration (relative to one or more flavors depending on the values of chemical po-
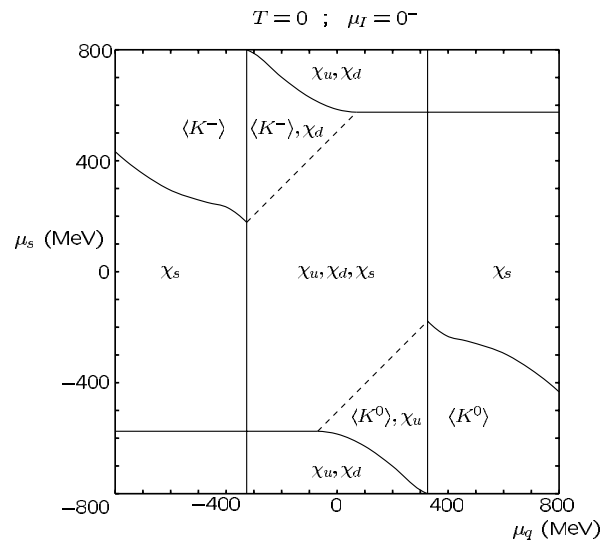

FIG. 7. Phase diagram for chiral symmetry restoration and kaon condensation in the plane (μ_q, μ_s) at $\mu_I = 0^-$ and $T = 0$. Different regions are specified by the nonvanishing of a given condensate, whereas the others are vanishing (ρ_{us}, ρ_{ds}) or order $\sim m_f/\Lambda$ (χ_u, χ_d, χ_s). Dashed lines are for the continuous vanishing of pseudoscalar fields, whereas solid lines are for discontinuous behaviors.
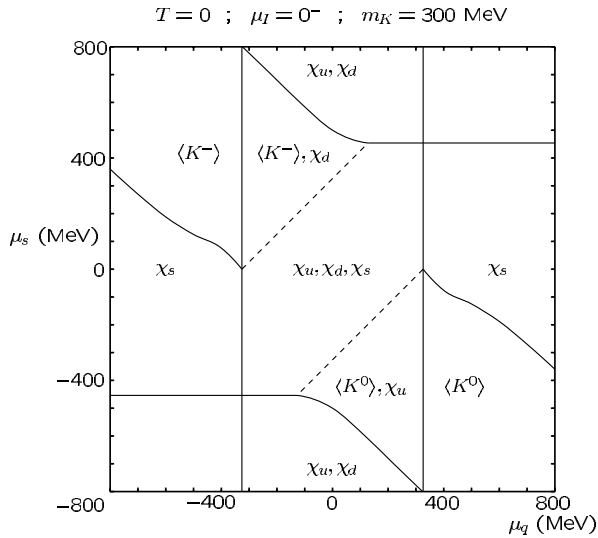
$$T = 0 \;\; ; \;\; \mu_I = 0^- \;\; ; \;\; m_K = 300 \text{ MeV}$$

FIG. 8. Phase diagram for chiral symmetry restoration and kaon condensation in the plane (μ_q, μ_s) at $\mu_I = 0^-$ and $T = 0$, and for $m_K = 300$ MeV. Different regions are specified by the nonvanishing of a given condensate, whereas the others are vanishing (ρ_{us}, ρ_{ds}) or order $\sim m_f/\Lambda$ (χ_u, χ_d, χ_s). Dashed lines are for the continuous vanishing of pseudoscalar fields, whereas solid lines are for discontinuous behaviors.

tentials) which are characterized by the respective scalar field $\chi_f \sim m_f/\Lambda$. Furthermore these regions are separated through discontinuous transitions, both from the normal phase and from the regions of kaon condensation. There are four different regions of this kind, distinguishable by the condensing kaon and by the values of the associated scalar condensates. Finally, the normal phase turns into a region of kaon condensation through the smooth rotation of χ_s and one of the light flavors (according to the sign of μ_Y one between χ_u or χ_d remains large) into a kaon condensate, when $\mu_Y \gtrsim m_K/2$, with a second order phase transition. We can see that the presence of a high value of $|\mu_q|$ lowers the corresponding $|\mu_s|$ necessary to have kaon condensation: moreover, a value of $\mu_I \neq 0$ would favor a

kaon condensation with lower values of $|\mu_q|$ and/or $|\mu_s|$. Since we do not know exactly the critical value μ_q^C for chiral symmetry restoration, and since we are interested here in the case where $\mu_q^C > m_K$, instead of varying μ_q^C (for instance performing a different fit) we take the kaon mass as a free parameter, by varying the strange quark mass, and we present, in Fig. 8, the same result as in Fig. 7, for $m_K = 300$ MeV, which is the upper limit for having a kaon condensation at $\mu_s = 0$.

V. CONCLUSIONS

In this paper we have presented a calculation of the QCD phase diagram obtained by using a 3-flavor NJL model. We have considered the plane (μ_I, μ_Y) to study the competition of kaon and pion condensation at zero and finite temperature and to establish a comparison with a previous analysis performed in a chiral model [20]. The results of the microscopical model accurately reproduce those achieved in the effective model only for low densities, since in the high strangeness density regime approximate chiral symmetry restoration (relative to the strange sector) occurs, disfavoring kaon with respect to pion condensation. Moreover we have suggested the possibility of kaon condensation driven only by light quark densities: this situation could be of interest in the core of compact stars, where the densities are approximatively associated only to light flavors. Up to now, we have neglected the possibility of di-quark condensation: however, we are currently working on an extension of this analysis that takes into account the superconductive phases too, so as to reproduce the physical picture proposed in the context of effective models for the K_0-CFL phase [22], and to understand the behavior of color superconductivity by varying arbitrarily the three quark chemical potentials [27]. Eventually, the inclusion of the β-equilibrium as well as charge and color neutrality, will give us a reasonable picture of cold quark matter within stars, and will make possible a comparison with experimental data.

[1] A. Barducci, R. Casalbuoni, S. De Curtis, R. Gatto, and G. Pettini, Phys. Lett. B **231**, 463 (1989); Phys. Rev. D **41**, 1610 (1990); Phys. Rev. D **46**, 2203 (1992); S.P. Klevansky, Rev. Mod. Phys. **64**, 649 (1992); A. Barducci, R. Casalbuoni, G. Pettini, and R. Gatto, Phys. Rev. D **49**, 426 (1994); T. Hatsuda and T. Kunihiro, Phys. Rep. **247**, 221 (1994); M. A. Halasz, A. D. Jackson, R. E. Shrock, M. A. Stephanov, and J. J. M. Verbaarschot, Phys. Rev. D **58**, 096007 (1998).

[2] A. Jakovac, A. Patkos, Zs. Szep, and P. Szepfalusy, Phys. Lett. B **582**, 179 (2004); hep-ph/0409076.

[3] M. Frank, M. Buballa, and M. Oertel, Phys. Lett. B **562**, 221 (2003).

[4] D. Toublan and J. B. Kogut, Phys. Lett. B **564**, 212 (2003).

[5] D. Toublan and J. B. Kogut, hep-ph/0409310.

[6] A. Steiner, M. Prakash, and J. M. Lattimer, Phys. Lett. B **486**, 239 (2000); A. W. Steiner, S. Reddy, and M. Prakash, Phys. Rev. D **66**, 094007 (2002); M. Buballa, hep-ph/0402234; F. Weber, Prog. Part. Nucl. Phys. **54**, 193 (2005); R. X. Xu, astro-ph/0407074.

[7] K. Rajagopal and F. Wilczek, *At the Frontier of Physics: Handbook of QCD*, Vol. 3, edited by M. Shifman, (World Scientific, Singapore, 2001), p. 2061; M. G. Alford, J. A. Bowers, J. M. Cheyne, and G. A. Cowan, Phys. Rev. D **67**,

054018 (2003).

[8] M. G. Alford, J. A. Bowers, and K. Rajagopal, Phys. Rev. D **63**, 074016 (2001).

[9] F. Neumann, M. Buballa, and M. Oertel, Nucl. Phys. A **714**, 481 (2003).

[10] M. Alford, C. Kouvaris, and K. Rajagopal, Phys. Rev. Lett., **92**, 222001 (2004).

[11] I. Shovkovy and M. Huang, Phys. Lett. B **564**, 205 (2003).

[12] Z. Fodor and S. D. Katz, J. High Energy Phys. 03 (2002) 014; J. High Energy Phys. 04 (2004) 050.

[13] P. de Forcrand and O. Philipsen, Nucl. Phys. B **642**, 290 (2002); Z. Fodor and S. D. Katz, Phys. Lett. B **534**, 87 (2002); C. R. Allton *et al.*, Phys. Rev. D **66**, 074507 (2002); M. D'Elia and M. P. Lombardo, Phys. Rev. D **67**, 014505 (2003).

[14] D. T. Son and M. A. Stephanov, Phys. Rev. Lett. **86**, 592 (2001).

[15] J. B. Kogut and D. K. Sinclair, Phys. Rev. D **66**, 014508 (2002); J. B. Kogut and D. K. Sinclair, Phys. Rev. D **66**, 034505 (2002); S. Gupta, hep-lat/0202005; D. K. Sinclair, J. B. Kogut, and D. Toublan, Prog. Theor. Phys. Suppl. **153**, 40 (2004); Y. Nishida, Phys. Rev. D **69**, 094501 (2004); D. N. Walters and S. Hands, hep-lat/0407034.

[16] K. Splittorff, D. T. Son and M. A. Stephanov, Phys. Rev. D **64**, 016003 (2001); M. Loewe and C. Villavicencio, Phys. Rev. D **70**, 074005 (2004); M. Loewe and C.

[17] B. Klein, D. Toublan, and J. J. M. Verbaarschot, Phys. Rev. D **68**, 014009 (2003).

[18] A. Barducci, G. Pettini, L. Ravagli, and R. Casalbuoni, Phys. Lett. B **564**, 217 (2003).

[19] A. Barducci, R. Casalbuoni, G. Pettini, and L. Ravagli, Phys. Rev. D **69**, 096004 (2004).

[20] J. B. Kogut and D. Toublan, Phys. Rev. D **64**, 034007 (2001).

[21] D. B. Kaplan and A. E. Nelson, Phys. Lett. B **175**, 57 (1986); H. D. Politzer and M. B. Wise, Phys. Lett. B **273**, 156 (1991); N. K. Glendenning and J. Schaffner-Bielich, Phys. Rev. Lett. **81**, 4564 (1998); S. Kubis and M. Kutschera, Acta Phys. Pol. B **30**, 2747 (1999).

[22] P. F. Bedaque, and T. Schafer, Nucl. Phys. A **697**, 802 (2002); T. Schafer, hep-ph/0304281; A. Kryjevski, D. B. Kaplan, and T. Schafer, hep-ph/0404290.

[23] P. Costa, M. C. Ruivo, Y. L. Kalinovsky, and C. A. de Sousa, Phys. Rev. C **70**, 025204 (2004).

[24] M. G. Alford, K. Rajagopal, and F. Wilczek, Phys. Lett. B **422**, 247 (1998); J. Berges and K. Rajagopal, Nucl. Phys. B **538**, 215 (1999).

[25] A. Barducci, R. Casalbuoni, S. De Curtis, D. Dominici, and R. Gatto, Phys. Rev. D **38**, 238 (1988).

[26] S. M. Schmidt, D. Blaschke, and Y. L. Kalinovsky, Phys. Rev. C **50**, 435 (1994).

[27] P. F. Bedaque, Nucl. Phys. A **697**, 569 (2002).